

## Magnetic and Crystallographic Transitions in the $\alpha$ - $\text{Mn}_2\text{O}_3$ - $\text{Fe}_2\text{O}_3$ System

R. W. GRANT, S. GELLER, J. A. CAPE, AND G. P. ESPINOSA

Science Center, North American Rockwell Corporation, Thousand Oaks, California

(Received 20 May 1968)

X-ray diffraction, Mössbauer spectroscopic, and magnetic susceptibility measurements have led to a determination of the phase diagram including magnetic phases of the system  $(\text{Mn}_{1-x}\text{Fe}_x)_2\text{O}_3$ ,  $0 \leq x \leq 0.63$ , the limit of  $\text{Fe}^{3+}$  cation solubility.  $\alpha$ - $\text{Mn}_2\text{O}_3$  itself is cubic (space group  $Ia3$ ) above 308°K and orthorhombic (space group  $Pcab$ ) below, the crystallographic transition being apparently higher than first order; it becomes antiferromagnetic at 79°K and at 25°K appears to go through a first-order transition to another antiferromagnetic structure. When 0.75 cation % of  $\text{Mn}^{3+}$  is replaced by  $\text{Fe}^{3+}$  ion, the lower transition occurs at 19°K. About 0.75%  $\text{Fe}^{3+}$  ion makes the structure cubic at room temperature; both the crystallographic and upper magnetic transition temperatures ( $T_t$  and  $T_{N1}$ , respectively) decrease monotonically and rather rapidly with increasing  $\text{Fe}^{3+}$  ion content. It is highly probable that when  $0.08 \lesssim x \lesssim 0.09$ ,  $T_{N1} = T_t$ ; when  $0.09 < x \leq 0.63$ , the structure apparently remains cubic down to 0°K and  $T_{N1}$  is almost independent of composition. X-ray powder data on  $\alpha$ - $\text{Mn}_2\text{O}_3$  at 6.5°K show no additional lines or symmetry change, implying that the transition at 25°K involves a shift in the symmetry center of the structure—a diffusionless but probably first-order transition; a change in space group is not required. Published neutron-diffraction data on  $\alpha$ - $\text{Mn}_2\text{O}_3$  and our own observations lead to the hypothesis that the magnetic space group of both orthorhombic phases is  $Pcab$  and of the cubic phase,  $Ia3$ . In the latter, the directions of the ordered spins of cations in the  $8b$  sites are absolutely fixed by symmetry, while those in  $24d$  sites are constrained to lie in planes perpendicular to the twofold axes. There are no symmetry restrictions on the spins in  $Pcab$ , but it is probable that all three magnetic structures are closely related. At all temperatures, the  $\text{Mn}^{3+}$  ions prefer the less symmetric  $24d$  sites, presumably because of the asymmetrical nature (Jahn-Teller distortion) of the electron distribution of the  $\text{Mn}^{3+}$  ion.

### I. INTRODUCTION

SEVERAL papers have appeared recently on magnetic and crystallographic studies of the  $\alpha$ - $\text{Mn}_2\text{O}_3$ - $\text{Fe}_2\text{O}_3$  system.<sup>1-5</sup> Early studies<sup>6-8</sup> showed that a continuous solid solution exists for the system  $(\text{Mn}_{1-x}\text{Fe}_x)_2\text{O}_3$  with  $0 \leq x \leq 0.6$ . Until recently, it was thought that the entire solid solution range was isostructural with bixbyite,  $(\text{Mn, Fe})_2\text{O}_3$ , which has the average symmetry of the space group  $Ia3$ . Structure analyses of bixbyite based on powder data have been reported.<sup>9</sup> The cations in this structure occupy two crystallographically nonequivalent sites, hereafter called  $d$  and  $b$  sites, with point symmetry  $2(24d)$  and  $\bar{3}(8b)$ , respectively. The room-temperature lattice parameter is almost independent of composition throughout the isostructural range. In a recent letter,<sup>10</sup> we reported

that at room temperature pure  $\alpha$ - $\text{Mn}_2\text{O}_3$  is not isostructural with bixbyite and has at most orthorhombic symmetry. This evidence was obtained from x-ray powder diffraction data. Single-crystal data have shown that  $\alpha$ - $\text{Mn}_2\text{O}_3$  is indeed orthorhombic at room temperature.<sup>11</sup> Since our preliminary reports on this work, Norrestam has reported<sup>12</sup> a crystal structure determination of orthorhombic  $\alpha$ - $\text{Mn}_2\text{O}_3$ .

In this paper we show that by a combination of techniques, namely, x-ray diffraction, Mössbauer spectroscopy, and magnetic susceptibility measurements, the phase diagram (including magnetic phases) has been determined and a relationship has been established between the upper Néel temperature  $T_{N1}$  and the crystal structure transformation temperature  $T_t$ . Because of some published neutron-diffraction data, we have also been able to draw some conclusions regarding the magnetic structures in the system. Some errors primarily associated with sample inhomogeneity have been reported in the literature and these are corrected in the present paper.

### II. EXPERIMENTAL

#### A. Apparatus Description

Lattice-constant measurements on single crystals were made with a Bond spectrometer.<sup>13</sup> Powder photographs at room temperature were taken with Norelco

<sup>1</sup> S. Geller, R. W. Grant, J. A. Cape, and G. P. Espinosa, J. Appl. Phys. **38**, 1457 (1967); also in Twelfth Annual Conference on Magnetism and Magnetic Materials, 1966 Paper No. U10 (unpublished).

<sup>2</sup> E. Banks and E. Kostiner, J. Appl. Phys. **37**, 1423 (1966).

<sup>3</sup> E. Banks, E. Kostiner, and G. K. Wertheim, J. Chem. Phys. **45**, 1189 (1966).

<sup>4</sup> R. R. Chevalier, G. Roullet, and E. F. Bertuat, Solid State Commun. **5**, 7 (1967).

<sup>5</sup> W. Hase and W. Meisel, Phys. Status Solidi **18**, K41 (1966).

<sup>6</sup> P. E. Wretblad, Z. Anorg. Allgem. Chem. **189**, 329 (1930).

<sup>7</sup> V. Montoro, Gazz. Chim. Ital. **70**, 145 (1940).

<sup>8</sup> B. Mason, Geol. Foren. Stockholm Forh. **65**, 95 (1943).

<sup>9</sup> L. Pauling and M. D. Shappell, Z. Krist. **75**, 128 (1930); H. Dachs, *ibid.* **107**, 370 (1956).

<sup>10</sup> S. Geller, J. A. Cape, R. W. Grant, and G. P. Espinosa, Phys. Letters **24A**, 369 (1967). The curve for 2%  $\text{Fe}^{3+}$  in Fig. 1 of this reference should be deleted. Unfortunately, the specimen was mislabeled; it is really one of  $\text{Mn}_3\text{O}_4$  containing 2 cation %  $\text{Fe}^{3+}$ . Further, the peak in this curve occurs at the same temperature as the  $T_{N1}$  for  $x \geq 0.09$ . This had led us to believe, erroneously, that only 2 cation %  $\text{Fe}^{3+}$  or less was required to reduce  $T_{N1}$  of  $\alpha$ - $\text{Mn}_2\text{O}_3$  by a factor of 2.

<sup>11</sup> S. Geller, R. W. Grant, J. A. Cape, and G. P. Espinosa, A.C.A. Winter Meeting, Paper No. D7, 1968 (unpublished); R. W. Grant, J. A. Cape, S. Geller, and G. P. Espinosa, Bull. Am. Phys. Soc. **13**, 462 (1968).

<sup>12</sup> R. Norrestam, Acta Chem. Scand. **21**, 2871 (1967).

<sup>13</sup> W. L. Bond, Acta Cryst. **13**, 814 (1960).

114.6-mm-diam cameras. Powder photographs obtained above room temperature were taken with a Bond camera<sup>14</sup> built in our laboratory. Low-temperature x-ray powder data were obtained with a Norelco camera which was specially modified for this purpose by P. B. Crandall. All powder photographs were taken with Cr *K* radiation. Buerger precession-camera photographs of single crystals were taken with Mo *K* radiation.

Mössbauer studies were performed on an automated mechanical cam-driven constant-velocity spectrometer in the normal transmission mode. The resonant radiation was the 14.4-keV  $\gamma$  transition in  $Fe^{57}$ . The source used for all measurements was  $Co^{57}$  in Cu at 23°C. All specimens were ground into fine powders in an agate mortar; the absorbers (specimens) used for the measurements were kept relatively thin to minimize saturation effects. Absorber temperatures other than room temperature were obtained in a cryogenic Dewar. The sample temperature was measured with a Au-2.1 at. % Co thermocouple attached to the Cu sample holder (with Be windows) and the temperature was held constant to  $\approx 0.5^\circ C$  by means of a temperature controller employing resistive heating.

Magnetization studies were performed by observation of the force on a container of randomly oriented crystals in an inhomogeneous magnetic field. Continuous data were taken as a function of temperature from liquid-helium to room temperature. In a typical experiment the field was a few kilogauss and the constant gradient was about 50 G/cm. A detailed description of the apparatus has already been given.<sup>15</sup>

### B. Sample Preparation

Difficulties in preparing homogeneous specimens throughout the  $(Mn_{1-x}Fe_x)_2O_3$  system have previously led to some erroneous conclusions. Our own previous studies<sup>1,10</sup> were made on specimens prepared by solid-state reaction techniques, used successfully on other systems in the past. However, in the  $Mn_2O_3$ - $Fe_2O_3$  system, for the high iron contents, it seemed necessary to fire the materials in the temperature range where the spinel was the stable phase<sup>16</sup>; otherwise, the  $\alpha$ - $Fe_2O_3$  would not completely "dissolve." The final firings were carried out in the temperature region where the  $\alpha$ - $Mn_2O_3$  phase was stable.<sup>16</sup> Firings were usually done in  $O_2$  atmosphere; however, it was found that in the vicinity of the phase boundaries there is some difference from firing in air.<sup>16</sup>

In the course of the measurements, results were obtained on low-iron-content specimens which were difficult to understand until we realized that, contrary to previous experience with other systems, the solid-state reaction did not produce homogeneous specimens, even with long annealing periods and a variety of heat treat-

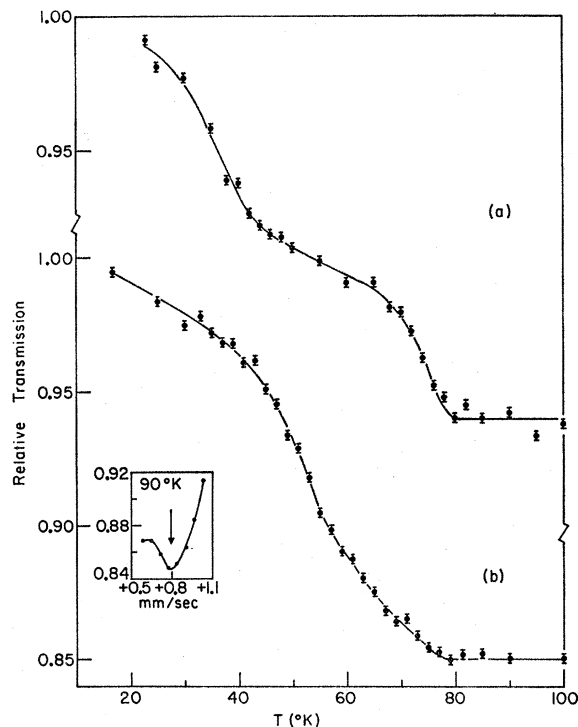


FIG. 1. Relative transmission at  $+0.79$  mm/sec versus temperature for a specimen  $(Mn_{0.948}Fe_{0.051})_2O_3$  prepared by solid-state reaction. (See text for details concerning the heat treatments given the specimen.) The insert shows the absorption line position (arrow) in the spectrum at  $90^\circ K$ .

ments (see also discussion at end of paper). The inhomogeneity was not that of the occurrence of undissolved  $Fe_2O_3$ , but rather of inhomogeneously dissolved  $Fe_2O_3$ . This could not be discerned in x-ray powder diffraction photographs because the lattice constant of the cubic phase (i.e., when  $x \geq 0.005$  at  $23^\circ C$ ) is very nearly independent of composition. Considering the treatments these specimens were given, it must be hypothesized that diffusion between particles was very slow after the initial solution occurred.

We have already indicated<sup>10</sup> the occurrence of inhomogeneity in these specimens, but we were also misled by it into believing that the replacement of between 1 and 2%  $Mn^{2+}$  by  $Fe^{3+}$  ions caused a discontinuous change in  $T_{N1}$ .

Because (as will be shown later) for  $x < 0.09$ ,  $T_{N1}$  decreases rapidly with  $x$ , the distribution of Néel temperatures can be detected by Mössbauer spectroscopy and used as an indicator of specimen inhomogeneity. This has already been partially demonstrated in Fig. 2 of Ref. 10. A further demonstration is given here.

Figure 1 shows the transmitted count rate versus temperature at a Doppler velocity of  $+0.79$  mm/sec. This resonance energy is near a maximum absorption associated with *d* site  $Fe^{3+}$  ions in the spectrum at  $90^\circ K$ , just above  $T_{N1}$ . (The insert in Fig. 1 gives the actual

<sup>14</sup> W. L. Bond, Rev. Sci. Instr. 29, 654 (1958).

<sup>15</sup> J. A. Cape, Phys. Rev. 132, 1486 (1963).

<sup>16</sup> A. Muan and S. Somiya, Am. J. Sci. 260, 230 (1962).

TABLE I. Lattice constant  $a$  at 23°C for cubic phases in  $(\text{Mn}_{1-x}\text{Fe}_x)_2\text{O}_3$  system.

$x$	$a$ (Å)	
	From powder photograph	Bond spectrometer
0.0075	9.413±0.001	
0.009	9.414	
0.017	9.414	9.4146±0.0001
0.028	9.414	
0.035	9.414	
0.060	9.415	
0.082	9.415	
0.097	9.415	9.4156±0.0002
0.49	9.415	9.4158±0.0002
0.63	9.412	9.4126±0.0003

line position.) The increase in the transmitted count rate as the temperature is lowered is caused by the onset of the magnetic hyperfine interaction. The two distinct breaks in the curve [Fig. 1(a)], similar to those of Fig. 2 of Ref. 10, are associated with the magnetic ordering of the iron-rich and the iron-deficient parts of the specimen. The specimen  $(\text{Mn}_{0.949}\text{Fe}_{0.051})_2\text{O}_3$  had received three firings (with regrinding and recompacting before each) at 945°C for a total of 37 h followed by a final firing at 600°C in air for 48 h. As shown in Fig. 1(b), the specimen was made somewhat more homogeneous by firing at 900°C seven times for a total of 240 h, followed by 50 h at 1200°C, 21 h at 800°C, and 16 h at 600°C again with regrinding and recompacting between firings. Although some improvement occurred as a result of all this, the specimen remained inhomogeneous: The distinct breaks of Fig. 1(a) were replaced by one very broad transition range [Fig. 1(b)]. Sharp transitions were obtained in specimens prepared by the techniques described below.

Two techniques produced homogeneous specimens in this system. A specimen (0.005 mole) containing 0.75 cation %  $\text{Fe}^{3+}$  was prepared by coprecipitation of the nitrates. Appropriate amounts of  $\text{MnCO}_3$  and iron metal isotopically enriched with  $\text{Fe}^{57}$  were dissolved in a minimum amount of dilute  $\text{HNO}_3$ . A few drops of dilute  $\text{H}_2\text{O}_2$  were added to dissolve the small amount of  $\text{MnO}_2$  formed. The solution was evaporated to dryness and heated to 300°C to decompose the nitrates. The resulting material was then thoroughly mixed in an agate mortar and pelletized. The pellet was placed in a platinum dish<sup>17</sup> and fired at 750°C for 1 h. The specimen was reground, repelletized, and refired nine times for a total duration of 450 h at temperatures between 960 and 400°C in an  $\text{O}_2$  atmosphere.

Because of the tedious nature of this method, we

decided to see what could be obtained from crystal-growing attempts. These attempts were successful and will be described separately by one of us (G.P.E.). Mössbauer measurements of the Néel temperature and low-temperature x-ray diffraction photography on specimens with  $x < 0.09$  showed that the specimens were homogeneous; for  $x < 0.09$ ,  $T_t$  is strongly dependent on  $x$  (see Sec. III A). The specimens with low iron concentration were partially isotopically enriched with  $\text{Fe}^{57}$  to facilitate the Mössbauer measurements. Standard chemical analysis was used to determine the actual Fe concentration in the single-crystal specimens. Throughout the remaining parts of this paper, data are reported only on specimens prepared by the single-crystal technique and the one specimen prepared by the coprecipitation technique.

### III. RESULTS

#### A. X-Ray Diffraction Studies

The powder x-ray diffraction data for  $\alpha\text{-Mn}_2\text{O}_3$  at room temperature were given in Ref. 10 (the line with  $d$  spacing 3.049 Å should be deleted). The lattice constants may be obtained to perhaps  $\pm 0.003$  Å from the three lines analogous to the cubic  $h^2+k^2+l^2=64$ . Thus,  $a=9.414$ ,  $b=9.424$ , and  $c=9.403\pm 0.003$  Å. Measurements on a single crystal with the Bond spectrometer<sup>13</sup> give  $a=9.4157$ ,  $b=9.4233$ ,  $c=9.4047\pm 0.0003$  Å at 23°C. At  $-75^\circ\text{C}$  the lattice constants determined from powder data are  $a=9.411$ ,  $b=9.448$ , and  $c=9.372\pm 0.003$  Å. The single-crystal x-ray data taken with a Buerger precession camera (Mo  $K$  radiation) show that  $\alpha\text{-Mn}_2\text{O}_3$  is orthorhombic and belongs to space group  $Pcab$ . This means that the manganese ions are in four sets of crystallographic positions of identity symmetry ( $8c$ ) or in three sets of identity symmetry ( $8c$ ) and two sets of  $\bar{1}$  symmetry. Norrestam<sup>12</sup> has refined the structure with the latter but apparently has not considered the former.

In an earlier report<sup>1</sup> based on materials prepared by solid-state reaction, we stated that the lattice constant of all compositions measured was  $9.414\pm 0.001$  Å. However, the measurements on single-crystal specimens with the Bond spectrometer do indicate very small but significant differences in lattice constant (see Table I).

Some years ago, it was shown from a study of the  $\text{Sc}_2\text{O}_3\text{-Fe}_2\text{O}_3$  system<sup>18</sup> that if  $\text{Fe}_2\text{O}_3$  were to have the bixbyite structure, its lattice constant would be 9.401 Å. This predicted value is in very good agreement with the value obtained for the  $\text{Mn}_2\text{O}_3$  saturated with  $\text{Fe}^{3+}$  ion (Table I). In a recent paper, Hase, Kleinstück, and Schulze<sup>19</sup> say (translated from the German) that according to Geller and co-workers its [meaning

<sup>18</sup> S. Geller, H. J. Williams, and R. C. Sherwood, *J. Chem. Phys.* **35**, 1908 (1961).

<sup>19</sup> W. Hase, K. Kleinstück, and G. E. R. Schulze, *Z. Krist.* **124**, 428 (1967).

<sup>17</sup> S. Geller, H. J. Williams, R. C. Sherwood, and G. P. Espinosa, *J. Phys. Chem. Solids* **23**, 1525 (1962).

hypothetically cubic  $Fe_2O_3$ ] lattice constant is approximately 0.2% smaller than that of  $\alpha$ - $Mn_2O_3$ . They also point out that Muan and Somiya<sup>16</sup> found first a slight expansion then contraction with increasing iron content. However, a difference of 0.2% was not reached, and therefore they assigned a lattice constant of 9.40 kX to both end members. Geller *et al.*<sup>18</sup> only made a comparison of the 9.410 Å predicted value with that reported by Mason,<sup>8</sup> 9.419 Å, an actual difference of only about 0.1%. It appears that Mason's value was high; the average value of the lattice constants of the orthorhombic unit cell is 9.415 Å (see above). The lattice-constant measurements (Table I) on single crystals do indicate a significant contraction at the saturation  $Fe^{3+}$  ion content.

Powder photographs taken above room temperature showed that at 38°C and above  $\alpha$ - $Mn_2O_3$  is cubic. We estimate the transition from the orthorhombic to the cubic structure to be at about 35°C. A plot of the lattice constant of cubic  $Mn_2O_3$  versus temperature to 430°C is shown in Fig. 2 as well as a similar plot for  $(Mn_{0.918}Fe_{0.082})_2O_3$  which remains cubic to temperatures below that of liquid nitrogen (see later discussion).

The crystallographic transition temperatures were determined both by low-temperature x-ray powder diffraction photography and Mössbauer spectroscopy (see next section). A plot of  $T_t$  ( $\pm 5^\circ C$ ) versus  $x$  is shown in Fig. 3(a). Extrapolation of the curve of  $T_t$  versus  $x$  to 0°K indicates that for  $x > 0.09$ , all solid solutions are cubic down to 0°K. The Néel temperatures  $T_{N1}$  determined by both magnetic susceptibility and Mössbauer spectroscopy (next two sections) are shown in Fig. 3(b). The insert in Fig. 3(b) shows the lower Néel temperature  $T_{N2}$  as determined by magnetic susceptibility. The plot of  $(T_t - T_{N1})$  versus  $x$  [Fig. 3(c)], when extrapolated to 0°K, shows that it is highly probable that  $T_{N1} = T_t$  for  $0.08 \lesssim x \lesssim 0.09$ .

### B. Mössbauer Studies

Mössbauer spectra were taken of several samples throughout the composition range and at various tem-

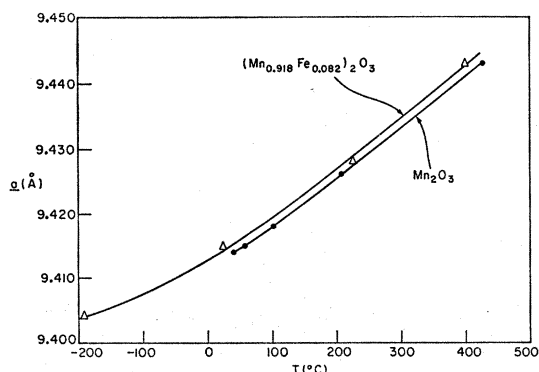


Fig. 2. Lattice constant versus temperature for  $Mn_2O_3$  and  $(Mn_{0.918}Fe_{0.082})_2O_3$ .

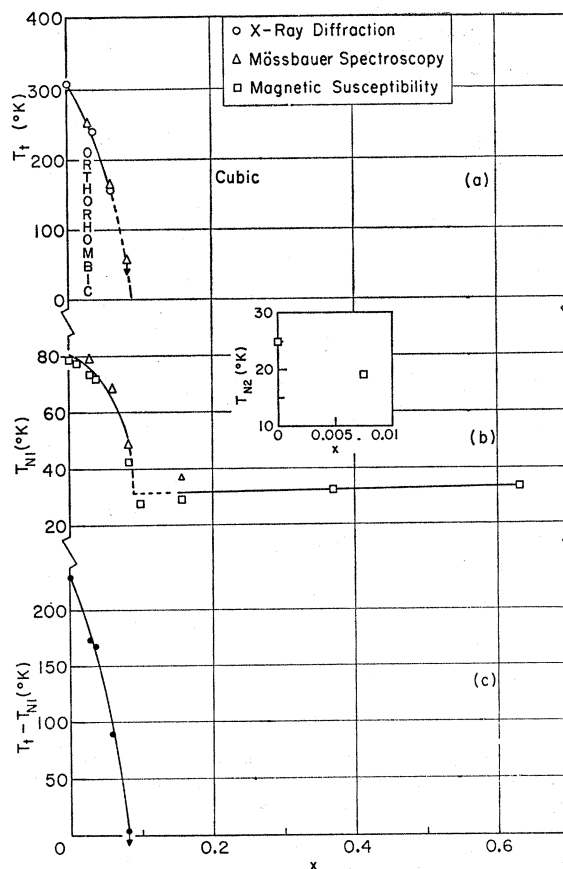


Fig. 3. Compositional dependence in the  $(Mn_{1-x}Fe_x)_2O_3$  system of (a) crystallographic transition temperature  $T_t$ ; (b) upper Néel temperature  $T_{N1}$  (insert shows  $T_{N2}$  versus  $x$ ); and (c)  $T_t - T_{N1}$ .

peratures. The room-temperature spectra (Fig. 4) of specimens with  $x = 0.060, 0.157,$  and  $0.33$ , annealed at  $800^\circ C$  in air for 15 h and air quenched, consist of two sets of partially resolved quadrupole split doublets associated with the two cation sites in the cubic phase. The lowest and highest energy lines are the quadrupole doublet associated with the more asymmetrical  $d$  sites while the inner set of lines is associated with the  $b$  sites. Because there are three times as many  $d$  sites as  $b$  sites, the assignment of the quadrupole doublets to the respective sites can be made unambiguously from the relative absorption intensities in the high-Fe-content specimens.<sup>3,5</sup> The same assignment may be made by associating the larger quadrupole splitting<sup>4</sup> with the more asymmetrical cation site. These spectra also show that the  $Fe^{3+}$  ions preferentially populate the  $b$  sites. The isomer shifts of the  $Fe^{3+}$  ions at both sites are nearly equal and are typical for the ionic  $Fe^{3+}$  ion. The absorption linewidths are considerably wider than natural width, which, as previously noted, is most likely associated with the statistical nature of the random solid solutions.<sup>3</sup>

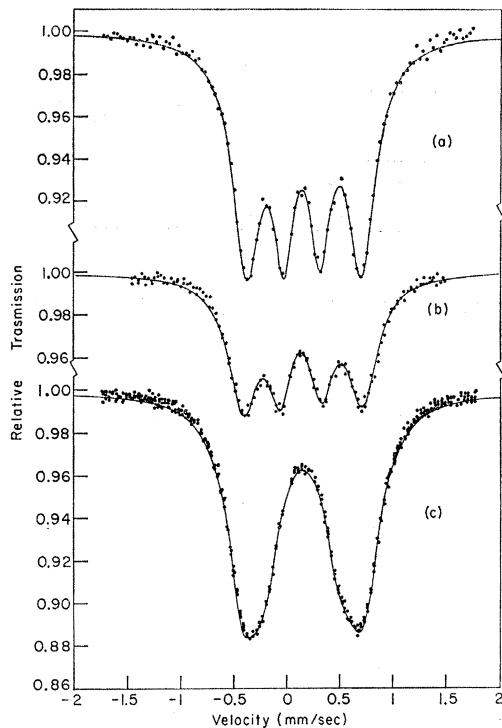


FIG. 4. Room-temperature Mössbauer spectra of  $(\text{Mn}_{1-x}\text{Fe}_x)_2\text{O}_3$  specimens annealed at  $800^\circ\text{C}$  in air for 15 h and air quenched (a)  $x=0.060$ , (b)  $x=0.157$ , (c)  $x=0.33$ .

Because  $\text{Fe}^{3+}$  is an  $S$ -state ion ( $^6S, 3d^5$ ), the principal contribution to the electric field gradient (EFG) observed at the Fe nucleus results from a noncubic charge distribution external to the ion itself modified by the Sternheimer factor,<sup>20</sup> which takes into account the core polarization of the ion. Thus, the temperature dependence of the quadrupole splitting (peak separation)  $\Delta E_Q$  observed in nearly all materials containing  $\text{Fe}^{3+}$  is small compared, for example, with that of materials containing  $\text{Fe}^{2+}$  ( $^5D$ ), which has low-lying electronic levels that are populated at ordinary temperatures. It follows that changes in  $\Delta E_Q$  observed at  $\text{Fe}^{3+}$  sites are primarily associated with changing charge distributions caused by structure distortions and thermal expansion. In Fig. 5, we show the variation of  $\Delta E_Q$  observed at the  $b$  and  $d$  sites,  $\Delta E_Q(b)$  and  $\Delta E_Q(d)$ , respectively, in the paramagnetic region for specimens with  $x=0.028, 0.060$ , and  $0.082$ . In the high-temperature region, the variation of both quadrupole splittings is very small in all specimens; however, for the two specimens with lower iron concentrations, this variation increases markedly below a specific temperature (shown by an arrow in the figure). This temperature corresponds to the onset of the orthorhombic distortion described in the previous section and agrees well with the transition temperatures determined

<sup>20</sup> R. M. Sternheimer, Phys. Rev. **130**, 1423 (1963).

by the low-temperature x-ray powder diffraction technique. The sample with  $x=0.082$  remains cubic to below  $55^\circ\text{K}$ . The increasing quadrupole splittings and increasing splitting of the high-angle x-ray diffraction lines show that the distortion increases continuously with decreasing temperature. For convenience, we shall continue to associate the larger  $\Delta E_Q$  with the  $d$  sites and the smaller  $\Delta E_Q$  with  $b$  sites even though below  $T_t$ ,  $\Delta E_Q(d)$  is really associated with three sets of crystallographically nonequivalent sites derived from the  $24d$  sites in the cubic phase, and it is possible that  $\Delta E_Q(b)$  is associated with two sets of sites in the orthorhombic structure.

In Figs. 6 and 7, we plot the variation of the isomer shift,  $\delta$ , and the average absorption linewidth  $\bar{\Gamma}$  for sites  $b$  and  $d$  as a function of  $T$  for the same three compositions as in Fig. 5. Again  $T_t$  is indicated by arrows in the figures. Within experimental error, there is neither a discontinuous change nor change in slope of any of the curves at  $T_t$ , suggesting that the crystallographic transition is of higher order than one. The variation of  $\delta_b$  and  $\delta_d$  in all cases seems attributable to the thermal red shift (second-order Doppler effect). The average linewidths of the two components of the quadrupole split doublets (Fig. 7) increase slightly as the temperature is lowered. Below  $T_t$ ,  $\bar{\Gamma}_d$  continues to broaden somewhat but apparently not at

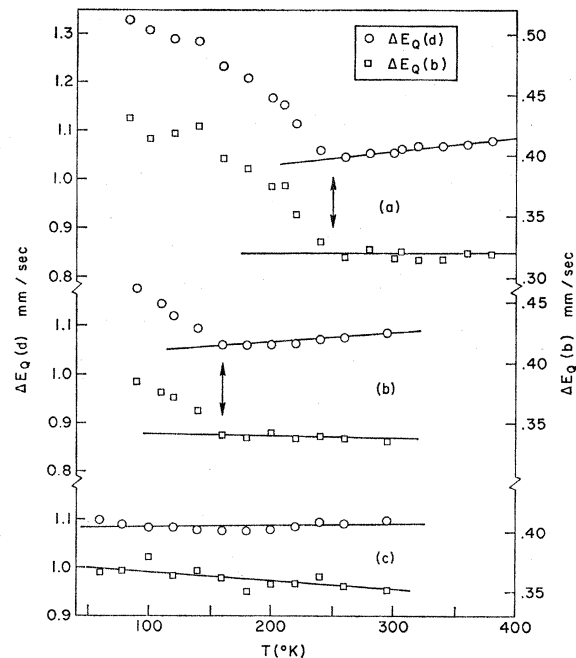


FIG. 5. Quadrupole splitting (peak separation) observed at  $\text{Fe}^{3+}$  ions in the  $8b$  and  $24d$  sites,  $\Delta E_Q(b)$  and  $\Delta E_Q(d)$ , respectively, as a function of temperature for specimens in the  $(\text{Mn}_{1-x}\text{Fe}_x)_2\text{O}_3$  system with (a)  $x=0.028$ , (b)  $x=0.060$ , (c)  $x=0.082$ . The crystallographic transition temperatures are indicated by arrows.

an increased rate. The relative constancy of  $\bar{\Gamma}_d$  below  $T_t$  suggests that at least the local environments of the 3 sets of sites generated from the  $24d$  sites of the  $Ia3$  structure do not differ much. Similarly, the cubic  $8b$  sites continue to be associated with a single set of resonance lines below  $T_t$ .

To determine  $T_{N1}$  of the specimens by Mössbauer spectroscopy, first a spectrum in the paramagnetic region just above  $T_{N1}$  was obtained. Then the absorption intensity of a maximum in the spectrum was measured

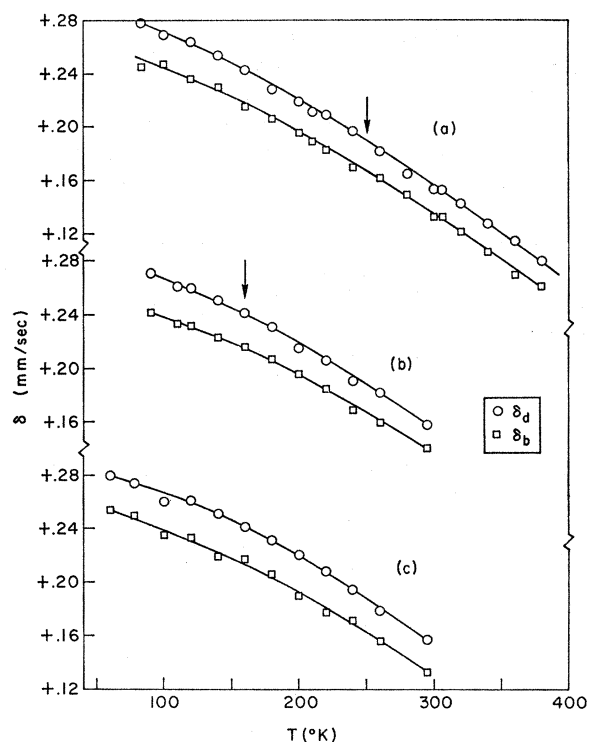


FIG. 6. Isomer shift observed at the  $Fe^{3+}$  ions in the  $8b$  and  $24d$  sites,  $\delta_b$  and  $\delta_d$ , respectively, as a function of temperature for specimens in the  $(Mn_{1-x}Fe_x)_2O_3$  system with (a)  $x=0.028$ , (b)  $x=0.060$ , (c)  $x=0.082$ . The crystallographic transition temperatures are indicated by arrows.

ured as the temperature was lowered;  $T_{N1}$  was the temperature at which the first significant decrease in absorption intensity (corresponding to the onset of a magnetic hfs interaction) occurred. An example of the results of this technique for  $(Mn_{0.94}Fe_{0.06})_2O_3$  is illustrated in Fig. 8. The absorption intensity at  $+0.855$  mm/sec corresponds to a line in the paramagnetic spectrum from the  $d$  sites (actually the sum of 3 sites) while  $+0.410$  mm/sec monitors the  $b$  sites. The first significant decrease in absorption for *both* sublattices occurs at about  $69^\circ K$ . Chevalier *et al.*<sup>4</sup> interpreted their data on similar compositions as implying two separate sublattice Néel temperatures which for this composition

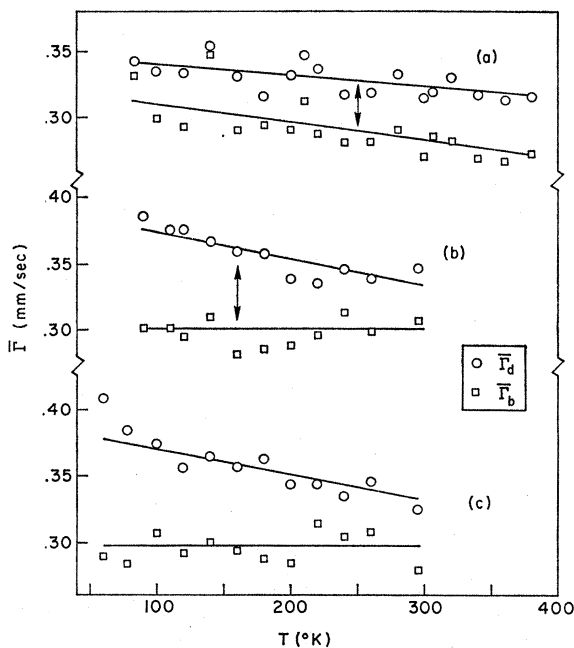


FIG. 7. The average Mössbauer absorption linewidths associated with the  $8b$  and  $24d$  sites,  $\bar{\Gamma}_b$  and  $\bar{\Gamma}_d$ , respectively, as a function of temperature for specimens in the  $(Mn_{1-x}Fe_x)_2O_3$  system with (a)  $x=0.028$ , (b)  $x=0.060$ , (c)  $x=0.082$ . The crystallographic transition temperatures are indicated by arrows.

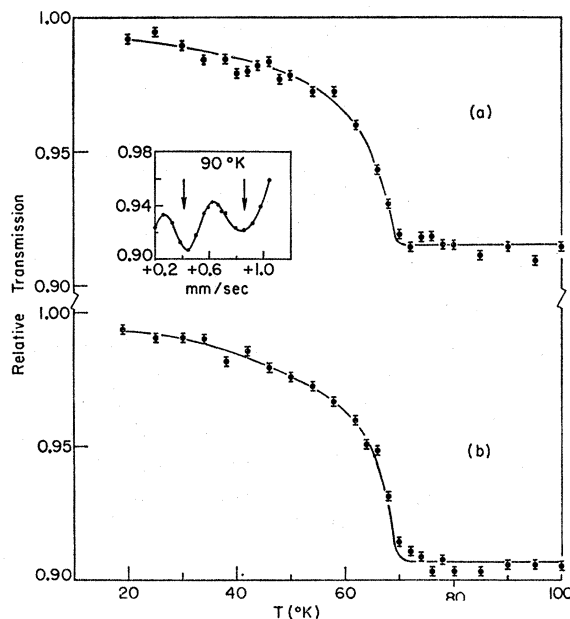


FIG. 8. Relative transmission at the Doppler velocities (a)  $+0.855$  mm/sec and (b)  $+0.410$  mm/sec as a function of temperature and for a specimen  $(Mn_{0.94}Fe_{0.06})_2O_3$ . The insert shows the absorption line positions (arrows) in the spectrum at  $90^\circ K$ .

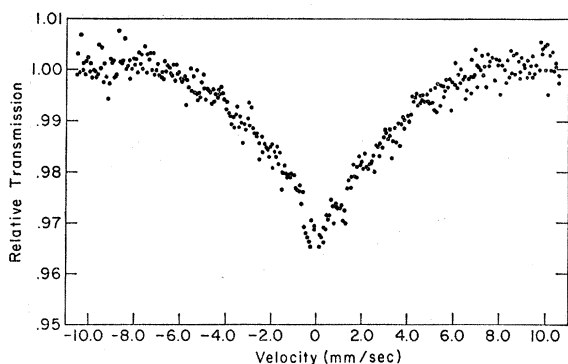
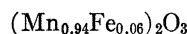


FIG. 9. Mössbauer spectrum of  $(\text{Mn}_{0.94}\text{Fe}_{0.06})_2\text{O}_3$  at  $55^\circ\text{K}$ .

would be  $\approx 66$  and  $28^\circ\text{K}$ . The spectrum of



at  $55^\circ\text{K}$ , shown in Fig. 9, demonstrates that the  $\text{Fe}^{3+}$  ion spins in both sublattices are ordered and that a distribution of hyperfine fields is present; Fig. 8 demonstrates that both sublattices have the same ordering temperature (to within experimental error,  $< 2^\circ\text{K}$ ). The observation of a central paramagnetic component in the Mössbauer spectrum below  $T_{N1}$  as observed by Chevalier *et al.*<sup>4</sup> and their hypothesis that different ordering temperatures occur in these materials for different magnetic sublattices undoubtedly result from inhomogeneity of their specimens (see Sec. II B).

### 1. Site Populations

As mentioned above and also shown by other investigators,<sup>3-5,19</sup> the  $\text{Fe}^{3+}$  ions preferentially populate  $b$  sites in the cubic structure. Because the orthorhombic modification is stable only near room temperature and below (Fig. 3) where ionic migration is extremely low, the  $\text{Fe}^{3+}$  will preferentially populate the sites in this structure derivable from the  $b$  sites of the cubic structure. As the iron concentration is increased (see Fig. 4), the  $b$  sites are increasingly filled so that more  $\text{Fe}^{3+}$  ions tend to enter  $d$  sites. In Fig. 10, we show two spectra, taken at  $23^\circ\text{C}$ , of the  $x=0.0075$  specimen which was (a) annealed at  $600^\circ\text{C}$  for 20 h in  $\text{O}_2$  and (b) annealed at  $960^\circ\text{C}$  for 24 h in  $\text{O}_2$ . After each annealing treatment, the specimen was quickly air cooled to room temperature. As expected, the spectra indicate that the more random distribution of  $\text{Fe}^{3+}$  between the two sites is obtained at the higher equilibrium temperature.

It is somewhat more edifying to consider the site preference of the  $\text{Mn}^{3+}$  ions because of the importance of these ions to the magnetic and crystal structures.<sup>10</sup> In the presence of the  $\text{Fe}^{3+}$  ions of *any* amount and at any temperature, the  $\text{Mn}^{3+}$  ions *always* prefer the lower symmetry sites (see also Refs. 3-5, 19). Presumably, this results from the asymmetrical nature of the electron distribution of the  $\text{Mn}^{3+}$  ion.<sup>10,19</sup>

To estimate the site energy difference (or more appropriately the enthalpy difference) for the  $\text{Fe}^{3+}$  ion (see also Ref. 21), we assume a Boltzmann distribution of the  $\text{Fe}^{3+}$  ions over the two sites and take into account the blocking of sites resulting from the preferential substitution. If the fractions of  $d$  and  $b$  sites which are occupied by  $\text{Fe}^{3+}$  ions are  $c_d$  and  $c_b$ , then

$$\exp(-\Delta/kT) = \frac{c_d(1-c_b)}{c_b(1-c_d)} = \frac{y(1+y-4x)}{3+y(3-4x)}, \quad (1)$$

where  $\Delta = (H_d - H_b)$  is the site enthalpy difference and  $T$  is the absolute temperature at which the site occupations were established (assumed equal to the annealing temperature). The distribution can also be expressed in terms of  $x$  and  $y$  where  $y = A_d/A_b = 3c_d/c_b$ , and  $A_d$  and  $A_b$  are the total Mössbauer absorption areas associated with sites  $d$  and  $b$ , respectively; note that  $x = \frac{1}{4}(3c_d + c_b)$ .

The absorption areas derived from Figs. 4 and 10, and other spectra, not shown, by least-squares fitting of the spectra to four Lorentz curves (solid lines in both figures) lead to  $\Delta = +0.059 \pm 0.005$  eV for compositions  $x \leq 0.1$  and for  $T \leq 800^\circ\text{C}$ . The value of  $\Delta$  may be temperature-dependent as indicated by a value of

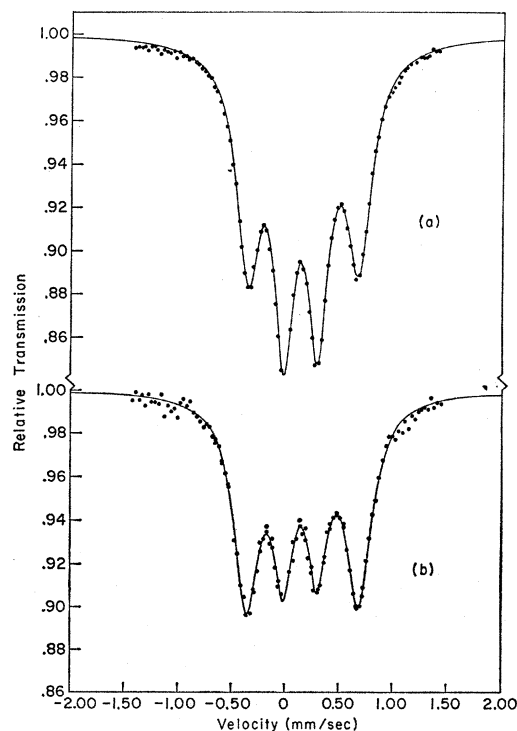


FIG. 10. Room-temperature Mössbauer spectra of  $(\text{Mn}_{0.9925}\text{Fe}_{0.0075})_2\text{O}_3$  following heat treatments of (a)  $600^\circ\text{C}$  for 20 h in  $\text{O}_2$  and (b)  $960^\circ\text{C}$  for 24 h in  $\text{O}_2$ .

<sup>21</sup> R. W. Grant, H. Wiedersich, S. Geller, U. Gonser, and G. P. Espinosa, *J. Appl. Phys.* **38**, 1455 (1967).

$\pm 0.090$  eV obtained from the  $x=0.0075$  specimen which was annealed to  $960^\circ\text{C}$  [Fig. 10(b)]. No detailed investigation of the possible temperature or compositional dependence of  $\Delta$  was made. At high Fe concentrations, the four absorption lines are very poorly resolved and it is therefore difficult to obtain accurate values for the site populations. However, we note that the site populations observed by Banks *et al.*<sup>3</sup> in  $(Mn_{0.5}Fe_{0.5})_2O_3$  lead to  $\Delta=+0.08$  eV (assuming an equilibrium  $T$  of  $750^\circ\text{C}$ ), which seems in reasonable agreement with the present result. Several minor assumptions are made in the above evaluation; in particular, we have assumed equal recoil-free fractions for all  $Fe^{3+}$  sites and neglected saturation corrections for these relatively thin absorbers. Thus, the absolute value of  $\Delta$  should be regarded only as a reasonable estimate.

### C. Magnetic Susceptibility Measurements

The "mass magnetic susceptibility" of five specimens from  $x=0$  to  $x=0.63$  is plotted versus  $T$  in Fig. 11. The "mass susceptibility"  $\chi_m$  is defined by

$$\chi_m = \chi d^{-1} = F[mH(dH/dx)]^{-1}, \quad (2)$$

where  $d$  is the density;  $\chi$ , the dimensionless susceptibility;  $F$ , the observed force;  $m$ , the total mass of the sample;  $H$  and  $dH/dx$ , the applied field and field gradient, respectively.

Some pertinent features of the data are as follows.

(1) For pure  $\alpha$ - $Mn_2O_3$  the shallow maximum at  $79$ – $80^\circ\text{K}$  is identified with the incipient antiferromagnetic ordering transition ( $T_{N1}$ ) in good agreement with

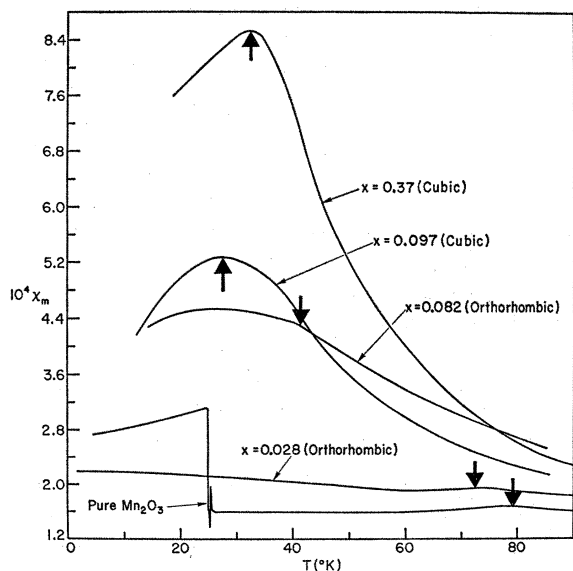


Fig. 11. Magnetic susceptibility versus temperature for five specimens in the  $(Mn_{1-x}Fe_x)_2O_3$  system.

the results of previous work.<sup>22,28</sup> In addition, a second magnetic transition apparently occurs at  $25^\circ\text{K}$  ( $T_{N2}$ ): the susceptibility changes by a factor of 2 in a discontinuous fashion. The same behavior is not observed in  $\alpha$ - $Mn_2O_3$  produced as a finely divided powder by solid-state reaction; however, a small peak does occur at about the same temperature, and it decreases to  $\approx 20^\circ\text{K}$  with the addition of 1%  $Fe^{3+}$  substitution<sup>10</sup> (see also Ref. 1). In the present study, we have also observed a discontinuous susceptibility at  $19^\circ\text{K}$  in a 0.75 cation %  $Fe^{3+}$  specimen prepared by the single-crystal technique, although the magnitude of the discontinuous change is much smaller than for the pure  $Mn_2O_3$  shown in Fig. 11.

(2) Two of the five curves shown in Fig. 11 are for samples which are in the cubic phase over the temperature range shown, while the other samples are orthorhombic. The latter exhibit a weak local maximum in the susceptibility indicated by the down-pointing arrows which we identify with  $T_{N1}$  [see also Fig. 3(b)]. The specimens with cubic structure ( $x=0.097$  and  $0.37$ ) exhibit only broad low-temperature maxima in  $\chi_m$  which very likely are indicative of magnetic transitions. While reminiscent of the low-temperature behavior reported earlier<sup>1</sup> for powder specimens with  $x \geq 0.20$  (for which the magnetic transitions were verified by Mössbauer studies), there are two differences: Unlike the specimens prepared by solid-state reaction, the single-crystal specimens do not exhibit the enhanced "frozen-in" susceptibility below the Néel point when cooled in a strong magnetic field. The other difference is the occurrence of shoulders in the  $\chi$ -versus- $T$  peaks for the high  $Fe^{3+}$  ion content specimens when prepared by solid-state reaction. A curve of this type is shown in Ref. 1 for  $(Mn_{0.5}Fe_{0.5})_2O_3$ . Both magnetic susceptibility and Mössbauer determinations of  $T_{N1}$  were made for a specimen with  $x=0.157$  [Fig. 3(b)]. The Mössbauer result was  $8^\circ\text{K}$  higher than the susceptibility value. Similar differences have been previously noted<sup>1</sup> and because this difference seems at least twice the limit of experimental uncertainty, it may indicate that the actual  $T_{N1}$  is slightly above the absolute maximum in the  $\chi_m$ -versus- $T$  curve in the cubic region. However, this difference is relatively small and the absolute value of  $T_{N1}$  in no way affects the conclusions drawn from the over-all shape of the  $T_{N1}$ -versus- $x$  curve.

From data such as those of Fig. 11, the dependence of  $T_{N1}$  on  $x$  determined by the relative maximum in  $\chi$  is shown plotted in Fig. 3(b). The data are consistent with the view that  $T_{N1}$  associated with the transition in the orthorhombic structure tends to a discontinuity at  $x=0.09$ , where the cubic structure becomes stable down to  $0^\circ\text{K}$ . In the cubic structure, the magnetic ordering temperature, if identified with the absolute

<sup>22</sup> E. G. King, J. Am. Chem. Soc. **76**, 3289 (1954).

<sup>28</sup> R. G. Meisenheimer and D. L. Cook, J. Chem. Phys. **30**, 605 (1959).



maximum in the susceptibility curves, appears to be only slightly dependent on  $x$ .

#### IV. DISCUSSION

##### A. Magnetic Space Groups

The magnetic structures of  $\alpha$ - $\text{Mn}_2\text{O}_3$  or any other members of the  $(\text{Mn}_{1-x}\text{Fe}_x)_2\text{O}_3$ ,  $x \leq 0.63$ , system have not been solved, although some preliminary neutron-diffraction studies have been reported.<sup>4,24</sup> If the paramagnetic-to-magnetic transition is assumed to be a single second-order phase transition (see Refs. 25 and 26), there will be symmetry restrictions on the spin arrangement of the cations in the magnetically ordered bixbyite structure. This is apparently the case in  $\text{Er}_2\text{O}_3$ , which has the bixbyite structure and orders magnetically in the magnetic space group  $Ia3$ .<sup>27</sup> The  $\text{Mn}^{3+}$  ions in  $\alpha$ - $\text{Mn}_2\text{O}_3$ , which is now known to belong to space group  $Pcab$ , are in either four sets of crystallographic positions of identity symmetry *or* in three sets of positions of identity symmetry and two of  $\bar{1}$  symmetry, and thus in either case have no symmetry restrictions on spin directions.

The magnetic susceptibility data of Fig. 11 and the neutron-diffraction data of Chevalier *et al.*<sup>4</sup> indicate a second magnetic structure for pure  $\alpha$ - $\text{Mn}_2\text{O}_3$  at low temperature, although there is some disagreement with our observation of the actual temperature associated with the onset of this second structure. Our present results indicate that  $T_{N2}$  is sharply decreased with increasing  $x$  [see insert in Fig. 3(b)]. (The observation of this transition was first reported in Ref. 1 and independently by Chevalier *et al.*<sup>4</sup>) The sharpness (Fig. 11) of this second magnetic transition indicates that it may be first order.

Powder diffraction data taken by P. Romo of  $\alpha$ - $\text{Mn}_2\text{O}_3$  at 6.5°K with  $\text{CrK}\alpha$  and with  $\text{FeK}\alpha$  radiation indicate that no change in symmetry occurs in this transformation. No new lines appear and, in particular, the {444} line remains unsplit. Of course, a change may occur that cannot be resolved by this technique, but assuming that the space group remains  $Pcab$ , there is a possible explanation.

As indicated earlier, Norrestam<sup>12</sup> assumed that the  $24d$  ions, with 2 symmetry, of the cubic phase go into three sets of  $8c$  ions of 1 symmetry in the orthorhombic phase, while the  $8b$  ions of  $\bar{3}$  symmetry in the cubic phase go into 2 sets,  $4a$  and  $4b$ , with  $\bar{1}$  symmetry in the orthorhombic phase. Such an arrangement gives three fewer

positional degrees of freedom than if the cubic  $8b$  ions also went into a set of  $8c$  sites. Even though the discrepancy factor attained in Norrestam's refinement is very low, he did not consider the latter alternative, and so we do not yet know whether its likelihood can be ruled out. Our guess would be that it cannot.

The two arrangements would, of course, give two different structures, Norrestam's with eight  $\text{Mn}^{3+}$  ions at  $\bar{1}$  symmetry sites and the alternative with no atoms at symmetry sites. We believe that if the structure between 25 and 308°K is one of these, then the other probably exists below 25°K, accounting for the transition as observed in the susceptibility data. The structures would still not be very different and the transition would be diffusionless, but could be first order. It involves a displacement of the symmetry center of the structure by  $(\frac{1}{4}, \frac{1}{4}, \frac{1}{4})$  and atomic displacements to conform to this shift. Because the magnetic structure includes the crystal structure, such a change implies a discontinuous change in spin arrangement also. However, again the two structures need not be, and probably are not, very different.

Mössbauer data with the 0.75 cation %  $\text{Fe}^{3+}$  specimen give an indication of a discontinuous change in the magnetic hyperfine spectrum associated with one set of sites at  $\sim 19^\circ\text{K}$ , which is consistent with the susceptibility result. Further Mössbauer measurements are planned to investigate this low-temperature transition.

Although there is uncertainty in the exact orthorhombic structure, the argument which follows makes it possible to predict the most probable magnetic space group for both orthorhombic  $\alpha$ - $\text{Mn}_2\text{O}_3$  and the bixbyite region of the  $(\text{Mn}_{1-x}\text{Fe}_x)_2\text{O}_3$  system. It should be pointed out that the uncertainty of the crystal structure does not affect the magnetic group: Both possibilities would belong to the same magnetic space group.

As described earlier, the crystal structure of  $\alpha$ - $\text{Mn}_2\text{O}_3$  ( $Pcab$ ) is a distortion of the bixbyite structure ( $Ia3$ ); all observations suggest that one structure goes into the other (as a function of  $T$ ) by a transition of higher order than 1. It seems very probable, therefore, that the magnetic structures of these two phases will be closely related. Our magnetic susceptibility data indicate that throughout the entire compositional region, the residual moment is  $\lesssim 0.01\mu_B$ , indicating antiferromagnetic ordering in all magnetic phases.

Strong {111} and {100} magnetic lines have been observed<sup>4,24</sup> in the neutron-diffraction data of  $\alpha$ - $\text{Mn}_2\text{O}_3$ , thus indicating a primitive magnetic unit cell. Assuming that the magnetic unit cell remains primitive in the higher-symmetry  $Ia3$  ( $x > 0.09$ ) structure, the most probable magnetic space group in this region is  $I_p a3$  (notation of Ref. 28) because the other two magnetic space groups derivable directly from  $Ia3$  ( $Ia3$  itself

<sup>24</sup> J. W. Cable, M. K. Wilkinson, E. O. Wollan, and W. C. Koehler, ORNL-2302, Physics Progress Report, 1957, p. 43. (unpublished).

<sup>25</sup> L. D. Landau and E. M. Lifshitz, *Statistical Physics* (Addison-Wesley Publishing Co., Inc., Reading, Mass., 1958), Chap. 14.

<sup>26</sup> J. O. Dimmock, *Phys. Rev.* **130**, 1337 (1963).

<sup>27</sup> E. F. Bertaut and R. Chevalier, *Compt. Rend.* **262B**, 1707 (1966).

<sup>28</sup> W. Opechowski and R. Guccione, in *Magnetism*, edited by G. T. Rado and H. Suhl (Academic Press Inc., New York, 1965), Vol. IIA, p. 105.

and  $Ia'3$ ) are both body centered. ( $Ia'3$  would also require the spins of atoms on  $b$  sites to be disordered.) The space group  $I_p a3$  leads to a unique spin arrangement for the cations on the  $b$  sites.<sup>29</sup> They are aligned antiparallel along body diagonals as shown in Fig. 12. However, the spins on the  $d$  sites are only confined to planes; all twofold rotation axes in the  $Ia3$  space group are antirotation axes in  $I_p a3$ . The  $d$  sites all lie on one of the mutually perpendicular  $2'$  axes and thus the spins of the  $d$ -site cations would be perpendicular to one of the  $2'$  axes (see Fig. 12).<sup>30</sup> The most closely related magnetic space group in the orthorhombic region of this system is then  $Pcab$  itself, and because the distortion from the cubic structure is small, we would speculate that the actual spin arrangement in  $Pcab$  is not very different from that in  $I_p a3$ .

### B. Possible Explanation of Low-Temperature Data on Solid-State Reaction Specimens

In our previous work<sup>1</sup> based on specimens prepared by solid-state reaction, we had shown for  $(Mn_{0.5}Fe_{0.5})_2O_3$  a  $\chi$ -versus- $T$  curve (see Fig. 1 of Ref. 1) which had a peak at  $\sim 38^\circ K$  and a shoulder at  $\sim 24^\circ K$ . Also, when the  $\chi$ -versus- $T$  measurements were made after having cooled the specimen in a field of 16 kOe, the susceptibility turned upward from the shoulder. Furthermore, there appeared to be a residual moment of  $\sim 0.01\mu_B$  at  $0^\circ K$ . We had thought that a second magnetic transition took place at the temperature of the shoulder and that below this temperature the material is a weak ferromagnet.

The single-crystal material did not give the same results as the ceramic material even after the crystals were (1) fired in  $O_2$  at  $960^\circ C$  for 48 h, (2) then finely ground and remeasured. However, (3) after pelletizing and refiring at  $900^\circ C$  for 4 h in  $O_2$ , a result similar to that for the ceramic was obtained: After cooling the specimen in a field of 16 kOe, with decreasing temperature,  $\chi$  stayed essentially constant. (For the ceramic,<sup>1</sup>  $\chi$  had risen substantially.)

In seeking an explanation of these observations, it seems that the effect of particle size is mainly to make the surface of the material more reactive. The experi-

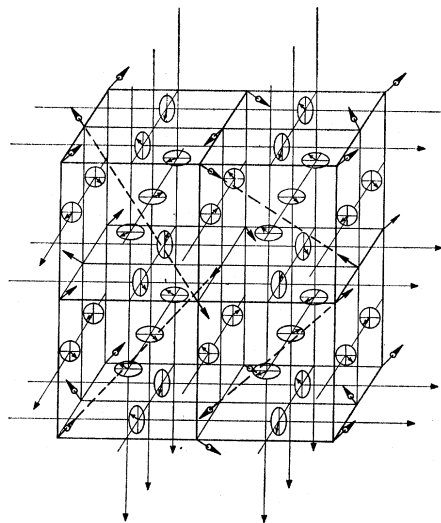


FIG. 12. Proposed magnetic structure for cubic phases belonging to  $I_p a3$ . Spin directions of cations on  $b$  sites are fixed along 3-fold axes as shown. Spin directions of cations on  $d$  sites lie in planes perpendicular to  $2'$ -fold axes. The spin directions on the  $d$  sites cannot be determined by the techniques used here, but must be related by the symmetry operators as shown.

ments indicate that it is unlikely that  $\chi$  versus  $T$  is directly particle-size-dependent.

The x-ray powder photographs from both crystals and ceramic showed no evidence of extraneous phases. Both gave expected lattice constants (Table I). No loss or gain of weight was observed in the described firings. However, it is probable that these firings resulted in either oxidation (or even reduction) of some of the  $Mn^{3+}$  ions at the particle surfaces. (Oxidation is more likely because of the existence of voids in the structure which could easily accommodate more anions.)

Because the observed magnetic effect is really not a large one, it is also probable that it is associated with slight unobservable structure changes resulting from the presence of minute amounts of Mn ions which are not trivalent.

### ACKNOWLEDGMENTS

We wish to thank B. Hickman for the use of and aid with his Bond spectrometer, P. Romo for making the powder diffractometer measurements at  $6.5^\circ K$ , D. H. Hern and S. A. Szabo for chemical analysis of the single-crystal specimens, and P. B. Crandall, M. Bloombaum, and D. H. Leslie for technical assistance.

<sup>29</sup> See, for example, the excellent article and bibliography of J. D. H. Donnay, *Trans. Assn.* **3**, 74 (1967).

<sup>30</sup> V. A. Koptsik, *Shubnikovskie Gruppy* (Moscow University Press, Moscow, 1966), was useful in preparing Fig. 12.